Supplementary Information

Optimizing cover crop practices as a sustainable solution for global agroecosystem services

Tianyi Qiu[1,2], Yu Shi[2], Josep Peñuelas[3,4], Ji Liu[5], Qingliang Cui[2], Jordi Sardans[3,4], Feng Zhou[6], Longlong Xia[7], Weiming Yan[2], Shuling Zhao[2], Shushi Peng[6], Jinshi Jian[2], Qinsi He[8], Wenju Zhang[9], Min Huang[1], Wenfeng Tan[10], Linchuan Fang[1,2,*]

[1] Key Laboratory of Green Utilization of Critical Non-metallic Mineral Resources, Ministry of Education, Wuhan University of Technology, Wuhan, China

[2] State Key Laboratory of Soil Erosion and Dryland Farming on the Loess Plateau, Institute of Soil and Water Conservation, Chinese Academy of Sciences, Yangling, China

[3] CSIC, Global Ecology Unit CREAF-CSIC-UAB, Bellaterra, Barcelona, Spain

[4] CREAF, Cerdanyola del Vallès, Barcelona, Spain

[5] State Key Laboratory of Loess and Quaternary Geology, Institute of Earth Environment, Chinese Academy of Sciences, Xi'an, China

[6] Sino-France Institute of Earth Systems Science, Laboratory for Earth Surface Processes, College of Urban and Environmental Sciences, Peking University, Beijing, China

[7] State Key Laboratory of Soil and Sustainable Agriculture, Institute of Soil Science, Chinese Academy of Sciences, Nanjing, China

[8] School of Life Sciences, Faculty of Science, University of Technology Sydney, PO Box 123, Broadway, Sydney, NSW 2007, Australia

[9] State Key Laboratory of Efficient Utilization of Arid and Semi-arid Arable Land in Northern China/Key Laboratory of Arable Land Quality Monitoring and Evaluation, Ministry of Agriculture and Rural Affairs, Institute of Agricultural Resources and Regional Planning, Chinese Academy of Agricultural Sciences, Beijing, China

[10] College of Resources and Environment, Huazhong Agricultural University, Wuhan, China

*** Corresponding author:** Linchuan Fang (flinc629@hotmail.com)

Supplementary Table 1 Results of mixed-effects model demonstrating the interaction of soil depth, initial SOC, and pH on the relative change of SOC stocks.

	Term	Estimated coefficient	95% CI
	Intercept	−0.3539 **	[−0.6196, −0.0881]
	Initial SOC	0.0274 **	[0.0086, 0.0461]
	pH	0.0651 ***	[0.0267, 0.1035]
Ln*RR* of SOC_{stock}~ Initial SOC*pH* Depth+(1|study/ID)	Depth	0.0429 ***	[0.0251, 0.0606]
	Initial SOC*pH	−0.0043 **	[−0.0071, −0.0014]
	Initial SOC*Depth	−0.0028 ***	[−0.0041, -0.0014]
	pH*Depth	−0.0066 ***	[−0.0092, -0.0040]
	Initial SOC*pH*Depth	0.0004 ***	[0.0002, 0.0006]

Note: *$P < 0.05$, **$P < 0.01$ and ***$P < 0.001$.

Supplementary Table 2 Multivariate mixed-effects model estimating the effects of environmental and management factors on agroecosystem multiservices in upland and paddy.

	Predictor	**Estimated coefficient**		**Predictor**	**Estimated coefficient**
Upland	MAT	0.1279	Paddy	MAT	0.5921
	MAP	0.0767		MAP	−0.8827
	Aridity index	−0.1232		Aridity index	**1.2702**
	BD	0.0178		BD	−0.0789
	Sand	**−0.2604**		Sand	−0.2572
	Clay	**−0.4301**		Clay	**−0.5748**
	Initial SOC	−0.1024		Initial SOC	**−0.4352**
	Soil C:N	**0.2180**		Soil C:N	**0.2884**
	pH	**0.1917**		pH	−0.1255
	Soil biodiversity	**0.4244**		Soil biodiversity	0.1137
	Microbial biomass	0.1500		Microbial biomass	0.2766
	F/B ratio	0.1143		F/B ratio	−0.1086
	N rate	**−0.0661**		N rate	−0.1184
	Organic fertilizer	**0.0945**		Organic fertilizer	**0.1661**
	Tillage	0.0270		Tillage	**−0.4602**
	Irrigation	**0.2500**		Irrigation	0.1427
	CC type	**0.0566**		CC type	−0.0067
	Residue management	**0.0941**		Residue management	**0.2722**
	CC diversity	−0.0233		CC diversity	**−0.3427**
	Duration	**0.2467**		Duration	0.0418
	CC growth days	0.0327		CC growth days	**−0.3210**
	CC termination time	**−0.0772**		CC termination time	0.0566

Note: Bold numbers represent significant estimated coefficients ($P < 0.05$).

Supplementary Table 3 List of global maps used for extracting missing values and scaling up.

Predictor	Unit	Original resolution	Year	Source
MAT	°C	1 km	1970–2000	WorldClim v2.1[1]
MAP	mm	1 km	1970–2000	WorldClim v2.1[1]
Aridity index	/	1 km	1970–2000	Global-AI_PET_ v3[2]
BD	g cm^{-3}	250 m	1950–2017	Soilgrids v0.2[3]
Sand	%	250 m	1950–2017	Soilgrids v0.2[3]
Clay	%	250 m	1950–2017	Soilgrids v0.2[3]
Initial SOC	g kg^{-1}	250 m	1950–2017	Soilgrids v0.2[3]
Soil C:N	/	1 km	1950–2017	Soilgrids v0.2[3]; Shangguan et al. (2014)[4]
pH	/	250 m	1950–2017	Soilgrids v0.2[3]
Soil biodiversity	/	0.1 degree	/	Orgiazzi et al. (2016)[5]
Microbial biomass	g C m^{-2}	0.5 degree	1961–2012	Xu et al. (2013)[6]
F/B ratio	/	0.5 degree	1970–2017	He et al. (2020)[7]
N rate	kg N ha^{-1}	5 arcmin	2000	Cui et al. (2021)[8]
Organic fertilizer	/	5 arcmin	2010–2019	Tian et al. (2022)[9]
Tillage	/	5 arcmin	2005	Porwollik et al. (2019)[10]
Irrigation	/	5 arcmin	2000	Cui et al. (2021)[8]
CC growth days	d	0.5 degree	2000	GGCMI Phase 3[11]; This study

Supplementary Table 4 Counting summary of experimental attributes and response variables across all CC studies included in the dataset.

	Category	***n***		**Category**	***n***
Country	Asia	7	Organic fertilizer	Yes	190
	Europe	11		No	2112
	Africa	2	Tillage	Conventional	1090
	Australia	1		Conservation	1212
	North America	2	Irrigation (upland)	Rainfed	1483
	South America	2		Irrigated	566
Cropland type	Upland	2049	Irrigation (paddy)	Rainfed	43
	Paddy	253		Flooding	135
Climate zone	Cold	911		Intermittent	75
	Temperate	1042	CC type	Legume	730
	Arid	290		Non-legume	1134
	Tropical	59		Mixture	438
Soil texture	Sandy	349	Residue management	Incorporated	1158
	Loam	1162		Surface	1012
	Clay loam	411		Removed	132
	Clay	380	Duration	<5 years	1518
Soil fertility	Low	769		≥5 years	784
	Moderate	769	Response variable	Yield	1149
	High	764		SOC_{stock}	1105
Soil pH	Acid	911		N_2O	363
	Neutral	933		CH_4	162
	Alkaline	458		MWD	376

Supplementary Table 5 The optimization of crop and soil parameters in the APSIM-Wheat model.

	Unit	Default value(s)	Adjusted value(s)	Relevance
Wheat parameters				
knh4	/	0.0	0.1	Ammonium nitrogen supply
minimum_grain_n_filling_rate	g/grain/d	0.000015	0.000014	Grain nitrogen demand
N_fact_photo	/	1.5	1.65	Nitrogen deficit effect on phenology
N_fact_expansion	/	1.0	21.5	Nitrogen deficit effect on expansion
N_fact_grain	/	1.5	1.6	Nitrogen deficit effect on grain
y_n_conc_crit_leaf	/	0.063 0.063 0.042 0.015 0.008 0.0035	0.047 0.05876 0.040 0.011 0.0462 0.0035	Critical leaf nitrogen concentrations
y_n_conc_max_leaf	/	0.070 0.070 0.050 0.020 0.010 0.005	0.070 0.070 0.050 0.020 0.050 0.005	Maximum leaf nitrogen concentrations
y_n_conc_crit_stem	/	0.050 0.050 0.020 0.010 0.005 0.0035	0.0485 0.0699 0.030 0.0035 0.00402 0.0035	Critical stem nitrogen concentrations
y_n_conc_max_stem	/	0.070 0.070 0.040 0.01 0.015 0.015	0.070 0.080 0.040 0.015 0.015 0.015	Maximum stem nitrogen concentrations
y_n_conc_min_pod	/	0.025 0.025 0.004 0.003 0.003 0.0025	0.025 0.025 0.004 0.009 0.00493 0.0025	Minimum pod nitrogen concentrations
n_conc_crit_root	/	0.020	0.0148	Critical root nitrogen concentrations
leaf_n_init_conc	/	0.050	0.0575	Initial leaf nitrogen concentration
leaf_n_sen_conc	/	0.005	0.0001	Senescent leaf nitrogen concentration
Soil parameters				
sw_top_crit	/	0.9	1.2	Critical water ratio in top soil layer
gravity_gradient	/	0.00002	0.000015	Vertical movement of soil moisture
nitrification_pot	ppm	40.0	6.0	Nitrification potential
nh4_at_half_pot	ppm	90	80	Half the maximum ammonium

Supplementary Table 6 Characteristics and predictive performance of five well-trained MF models after 10-fold cross-validation.

Response variable	**Weight**	**Mtry**	**Node size**	$\boldsymbol{R^2_{oob}}$	**MAE**
Yield	unif	6	1	0.638	0.121
SOC stock	fixed	3	6	0.327	0.073
N_2O	unif	6	6	0.362	0.404
CH_4	random	1	6	0.220	0.515
MWD	unif	6	6	0.478	0.110

Note: Mtry and node size represent the number of variables used for binary tree in the node and minimum node size, respectively. MAE and R^2_{oob} denote the mean absolute error and out-of-bag R^2.

Supplementary Table 7 Global datasets of cropland area and the related baselines of five agroecosystem services.

	Unit	**Original resolution**	**Year**	**Source**
Cropland area	/	5 arcmin	2000	MIRCA2000[12]
Crop yields	kg ha^{-1}	5 arcmin	1970-2000	SPAM2010[13]
SOC stocks	kg m^{-2}	250 m	1970-2000	Soilgrids v0.2[3]
N_2O emissions	kg m^{-2} s^{-1}	1 km	1970-2019	EDGAR v7.0[14]
CH_4 emissions	kg m^{-2} s^{-1}	250 m	1970-2019	EDGAR v7.0[14]
Soil erosion	Mg ha^{-1} yr^{-1}	100 m	2019	GloSEM[15]

Supplementary Table 8 Five bias-corrected CMIP6 model outputs provided by ISIMIP3b for projecting the CC benefits under the SSP126 and SSP370 scenarios (2021–2030, 2041–2050, 2061–2070, and 2091–2100).

	Affiliation	**Resolution**	**Climate sensitivity**
GFDL-ESM-4	Geophysical Fluid Dynamics Laboratory, National Oceanic and Atmosphere Administration (USA)	0.5°, daily	High
IPSL-CM6A-LR	Institute Pierre Simon Laplace (France)	0.5°, daily	Low
MPI-ESM1-2-HR	Max Planck Institute for Meteorology (Germany)	0.5°, daily	High
MRI-ESM2-0	Meteorological Research Institute, Japan Meteorological Agency (Japan)	0.5°, daily	High
UKESM1-0-LL	National Centre for Atmospheric Science and Met Office Hadley Centre (UK)	0.5°, daily	Low

References

1. Fick, S. E., & Hijmans, R. J. WorldClim 2: new 1-km spatial resolution climate surfaces for global land areas.In. *J. Climatol*. **37**, 4302–4315 (2017).
2. Zomer, R. J., Xu, J., & Trabucco, A. Version 3 of the global aridity index and potential evapotranspiration database. *Sci. Data* **9**, 409 (2022).
3. Hengl, T. et al. SoilGrids250m: Global gridded soil information based on machine learning. *PLoS ONE* **12**, e0169748 (2017).
4. Shangguan, W., Dai, Y., Duan, Q., Liu, B., & Yuan, H. A global soil data set for earth system modeling. *J. Adv. Model. Earth Sy*. **6**, 249–263 (2014).
5. Orgiazzi, A., Bardgett, R. D., & Barrios, E. Global soil biodiversity atlas. (European Commission, 2016).
6. Xu, X., Thornton, P. E., & Post, W. M. A global analysis of soil microbial biomass carbon, nitrogen and phosphorus in terrestrial ecosystems. *Global Ecol. Biogeogr.* **22**, 737–749 (2013).
7. He, L. et al. Global biogeography of fungal and bacterial biomass carbon in topsoil. *Soil Biol. Biochem.* **151**, 108024 (2020).
8. Cui, X. et al. Global mapping of crop-specific emission factors highlights hotspots of nitrous oxide mitigation. *Nat. Food* **2**, 886–893 (2021).
9. Tian, H. et al. History of anthropogenic Nitrogen inputs (HaNi) to the terrestrial biosphere: a 5 arcmin resolution annual dataset from 1860 to 2019. *Earth Syst. Sci. Data* **14**, 4551–4568 (2022).
10. Porwollik, V., Rolinski, S., Heinke, J., & Müller, C. Generating a rule-based global gridded tillage dataset. *Earth Syst. Sci. Data* **11**, 823–843 (2019).
11. Jägermeyr, J. et al. Climate impacts on global agriculture emerge earlier in new generation of climate and crop models. *Nat. Food* **2**, 873–885 (2021).
12. Portmann, F. T., Siebert, S., & Döll, P. MIRCA2000—Global monthly irrigated and rainfed crop areas around the year 2000: A new high-resolution data set for agricultural and hydrological modeling. *Global Biogeochem. Cy.* **24**, GB1011 (2010).
13. Yu, Q. et al. A cultivated planet in 2010–Part 2: The global gridded agricultural-production maps. *Earth Syst. Sci. Data* **12**, 3545–3572 (2020).
14. Crippa, M. et al. GHG emissions of all world countries. Publications Office of the European Union. https://publications.jrc.ec.europa.eu/repository/handle/JRC126363 (2021).
15. Borrelli, P., Ballabio, C., Yang, J. E., Robinson, D. A., & Panagos, P. GloSEM: High-resolution global estimates of present and future soil displacement in croplands by water erosion. *Sci. Dat*a **9**, 406 (2022).

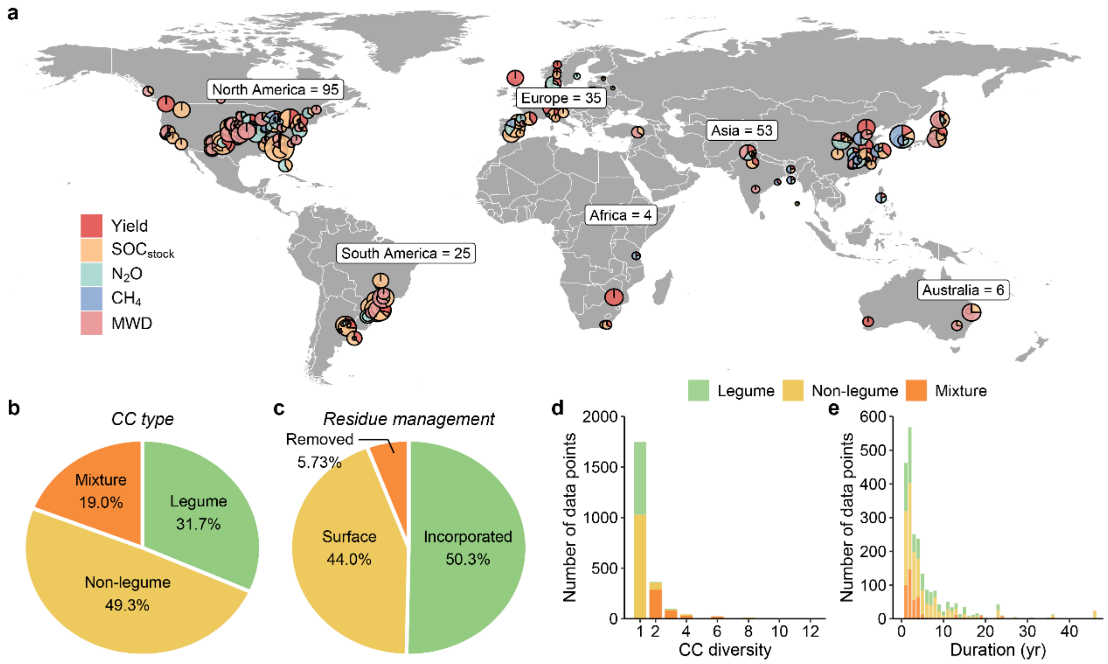

Supplementary Figure 1 Study sties and historical CC practice options. (a) Global distribution of study sites (*n* = 218). Pie charts show the observations and proportions of five agroecosystem services (yields, SOC stocks, N_2O emissions, CH_4 emissions, and MWD) at each site. Proportions of CC type (b) and residue management (c) adopted in historical CC practices. Numbers of observations in CC diversity (d) and implementation duration (e), with their fractions divided by different CC types.

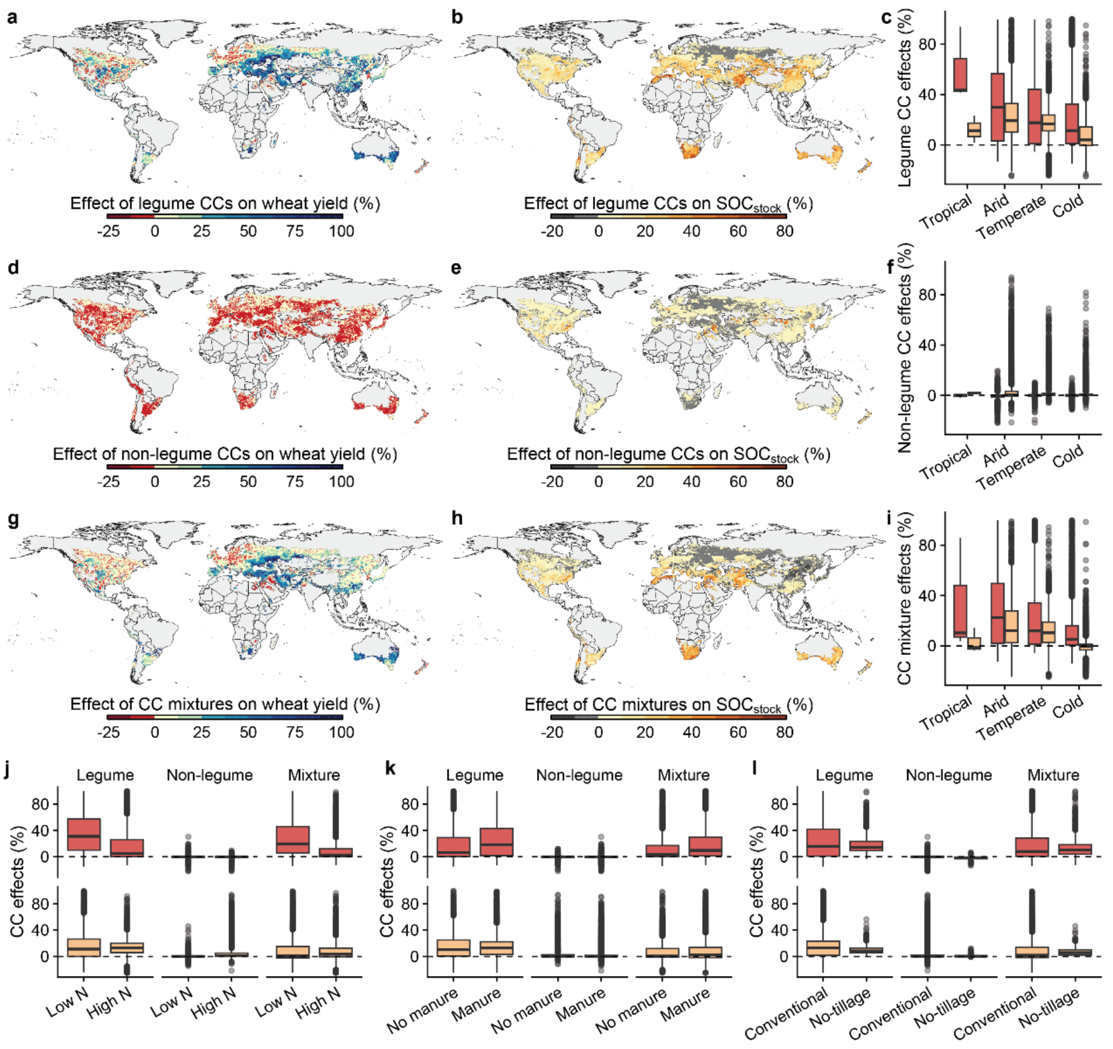

Supplementary Figure 2 APSIM results verifying the benefits (%, 40-year average) of CC practices for global major crop (wheat) yields (a, d, g) and SOC stocks (b, e, h) from 1981 to 2020. Boxplots show the median, 25th and 75th percentiles, and outliers of yields (red color) and SOC stocks (yellow color) in each climate zone (c, f, i), or under each N fertilizer rate (j), use of manure (k), and tillage (l). Boxplots show the median (center line), the interquartile range between the first and third quartiles (box bounds), whiskers extending to 1.5 times the interquartile range from the quartiles, and any points beyond this range as outliers. The classification of climate zones is according to the Köppen-Geiger climate classification. Low N and high N denote ≤ 100 kg N ha^{-1} and > 100 kg N ha^{-1}, respectively.

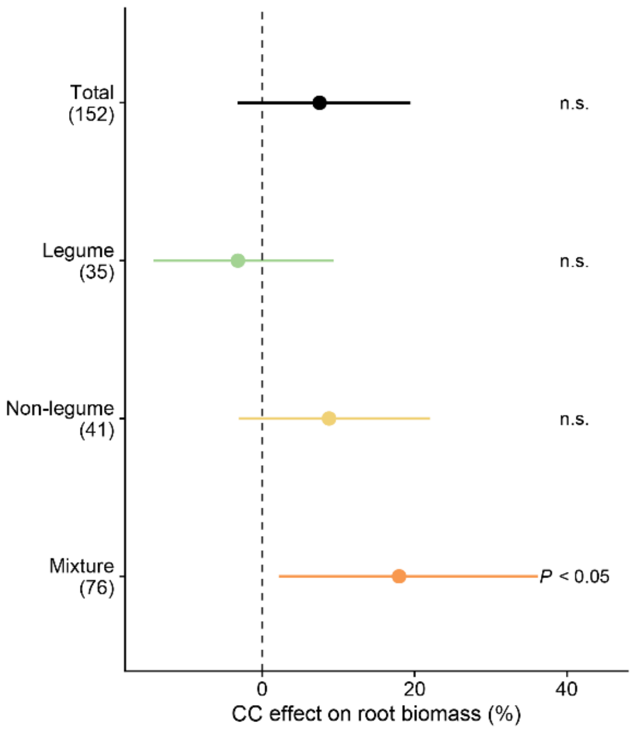

Supplementary Figure 3 Varied CC effects on root biomass among different CC types. Dots represent the weighted CC effect sizes and their 95% confidence intervals. Numbers in brackets indicate the number of observations. n.s., not significant. Source data are provided as a Source Data file.

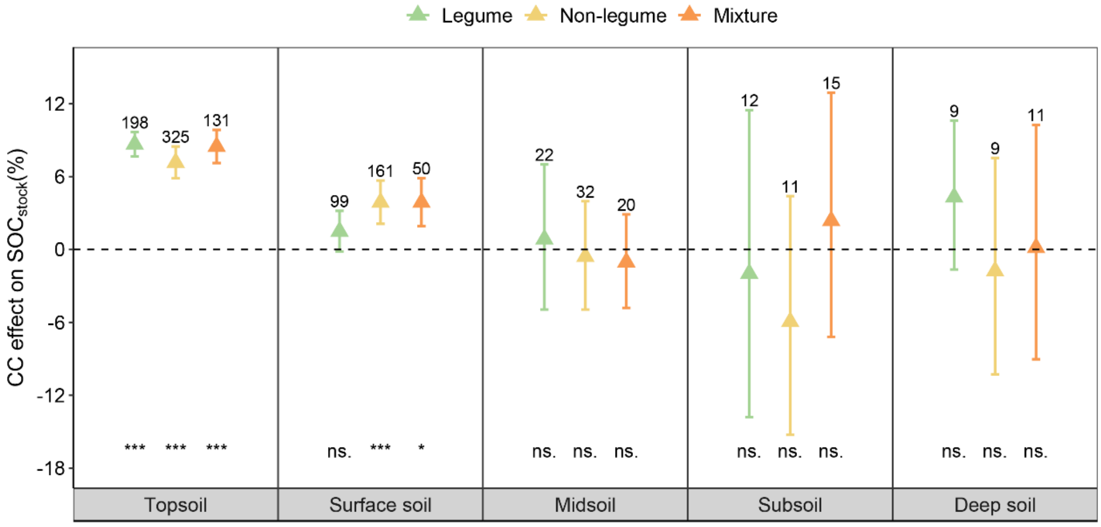

Supplementary Figure 4 Effects of different types of CCs on SOC stocks across soil layers, including topsoil (0–10 cm), surface soil (10–30 cm), midsoil (30-60 cm), subsoil (60-100 cm), and deep soil (>100 cm). Triangles represent the weighted CC effect sizes and their 95% confidence intervals. Numbers above the error bars indicate the number of observations. *$P < 0.05$ and ***$P < 0.001$; n.s., not significant.

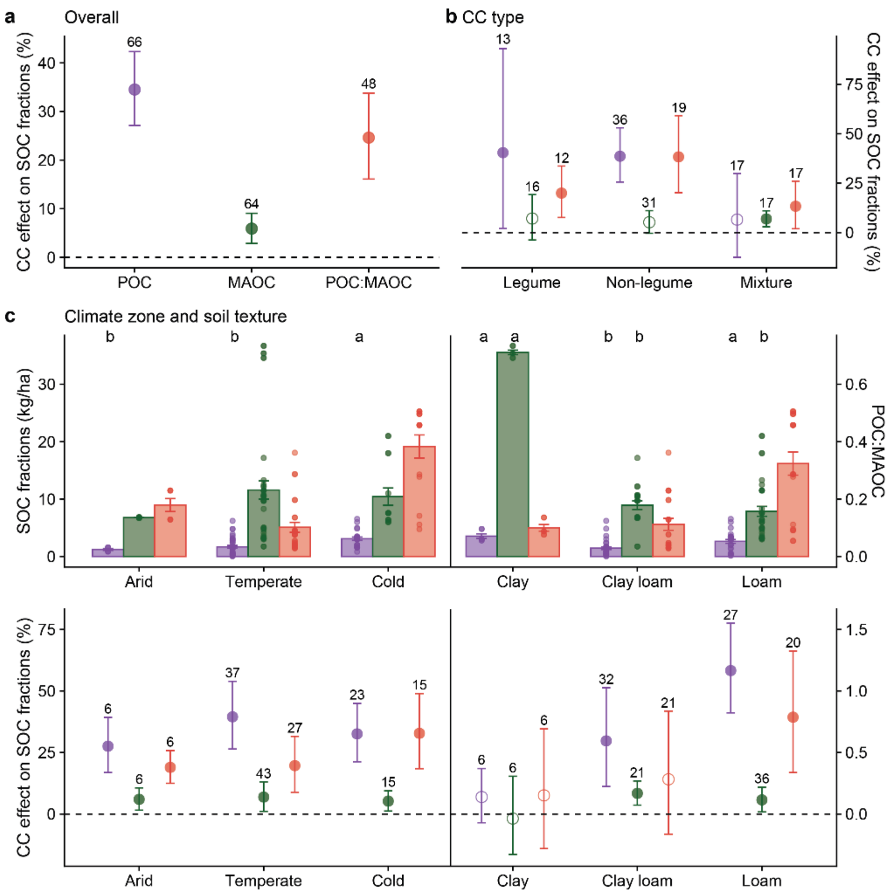

Supplementary Figure 5 Long-term effects of CCs on SOC fractions (a) and their variations under different CC types (b), climates and soil types (c). Dots represent the weighted CC effect sizes and their 95% confidence intervals. Solid and empty dots indicate significant and non-significant changes, respectively. Numbers above error bars denote the number of observations. Bars in (c) indicate the initial concentrations or ratios of SOC fractions (means ± standard error), with different lowercase letters indicating significant differences ($P < 0.05$) among climate zones or soil types. Multiple comparison for SOC fractions of different groups has been tested using Wilcoxon test. POC, particulate organic C; MAOC, mineral-associated organic C; POC:MAOC, the ratio of particulate organic C to mineral-associated organic C. Source data are provided as a Source Data file.

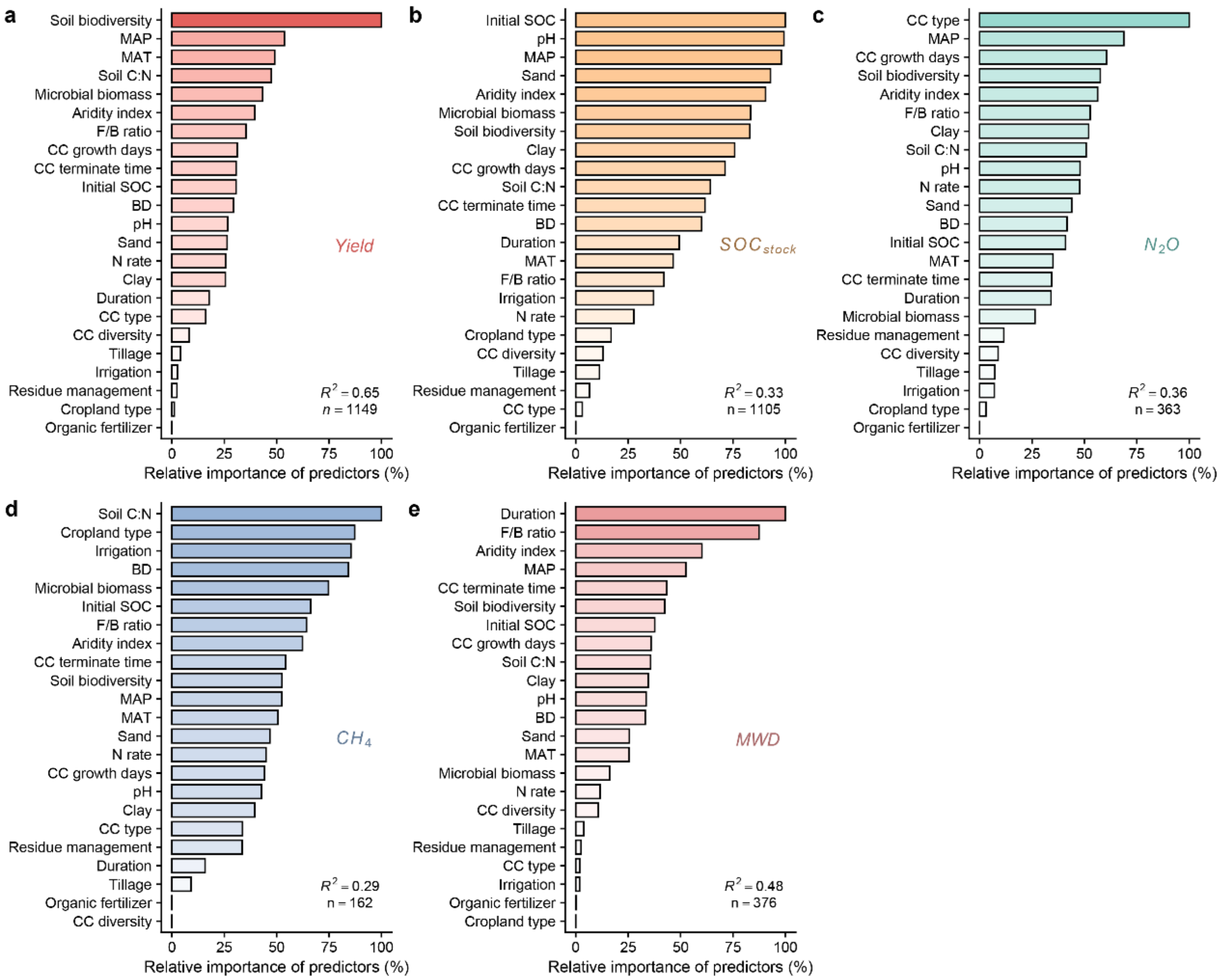

Supplementary Figure 6 MF-model-based relative importance of predictors for CC effects on five agroecosystem services, including yield (a), SOC stock (b), N_2O (c), CH_4 (d), and MWD (e). Bars filled with darker colors denote higher importance of predictors within each response variable. R^2 refers to the variance explained by each model based on 10-fold cross-validation.

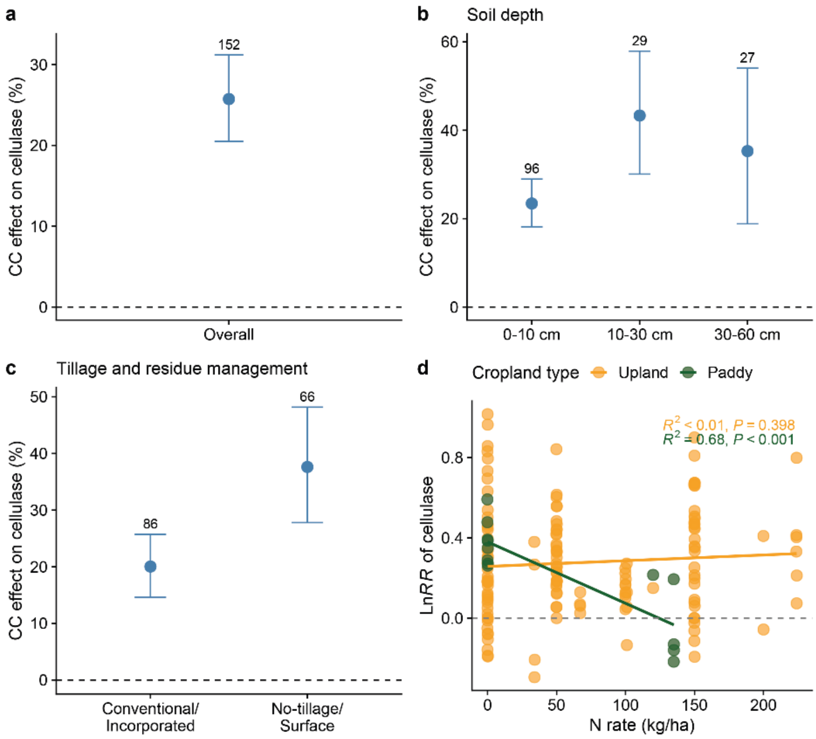

Supplementary Figure 7 Responses of cellulase activity along soil profiles to long-term CC practices (a, b) with tillage and fertilizer management (c, d). Dots indicate the weighted CC effect sizes and their 95% confidence intervals. Numbers above error bars denote the number of observations. Colors in (d) represent cellulase responses in different cropland types. Source data are provided as a Source Data file.

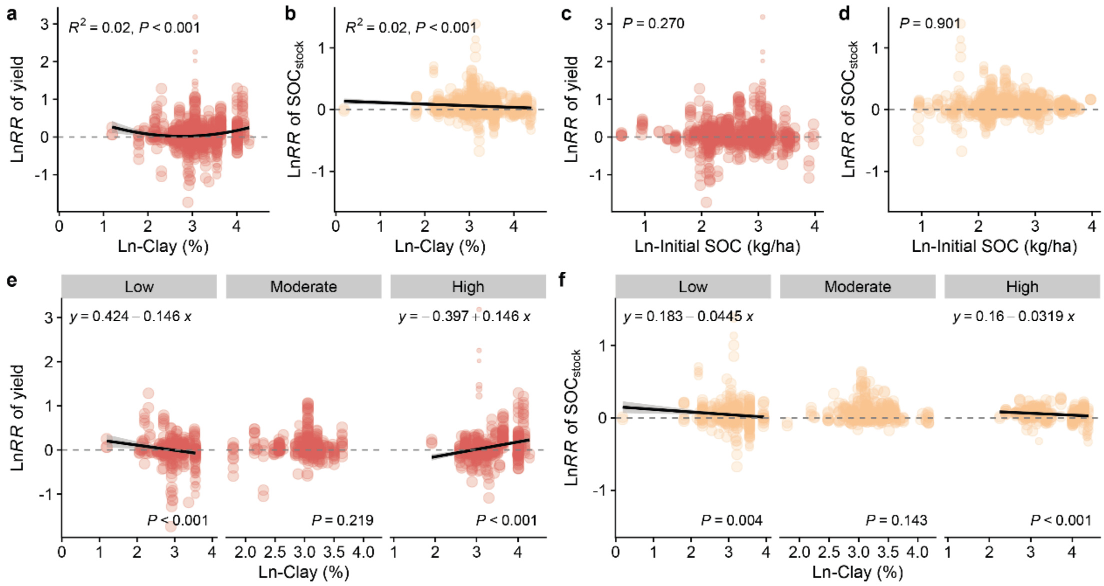

Supplementary Figure 8 Mutual control of soil texture and fertility on the relative changes in yields and SOC stocks (ln*RR*s). Relationship between ln*RR*s and soil clay content (a, b) or initial SOC concentration (c, d). Differential relationship between ln*RR*s and soil clay content among soil fertility groups (e, f). Black solid lines denote the significant correlations, with dot sizes proportional to model weights. Source data are provided as a Source Data file.

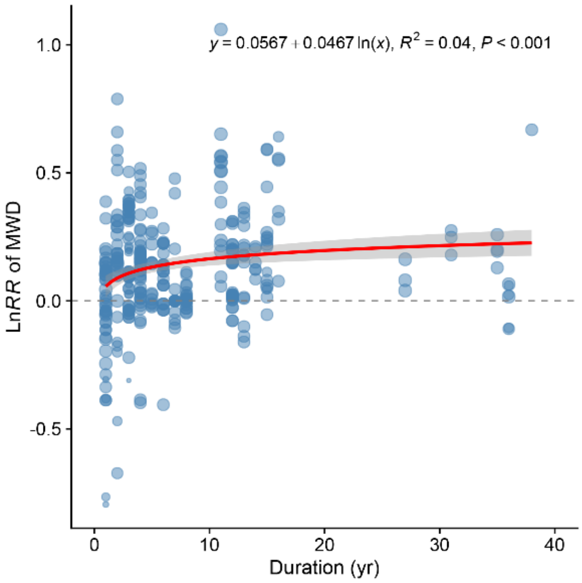

Supplementary Figure 9 Continuously enhanced CC improvement of MWD with the extending experimental duration. Red solid line denotes the significant logarithm correlation, with dot sizes are the scaling of model weights. Source data are provided as a Source Data file.

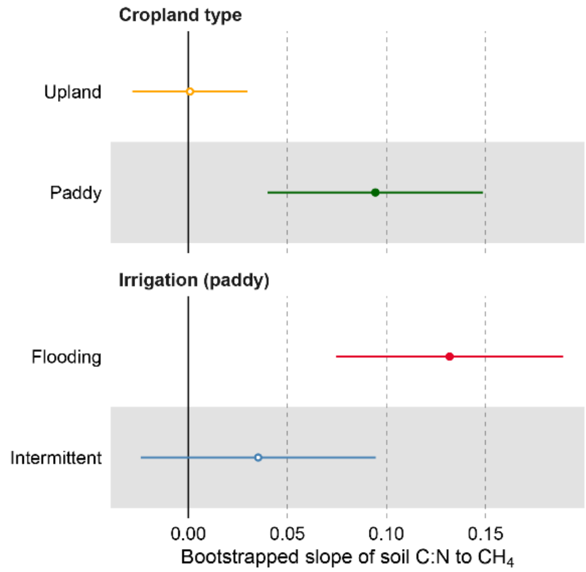

Supplementary Figure 10 Joint control of cropland type and irrigation method on the bootstrapped slope of soil C:N versus CH_4 change. Dots indicate the weighted CC effect sizes and their 95% confidence intervals. Solid and empty dots indicate significant and non-significant changes, respectively. Source data are provided as a Source Data file.

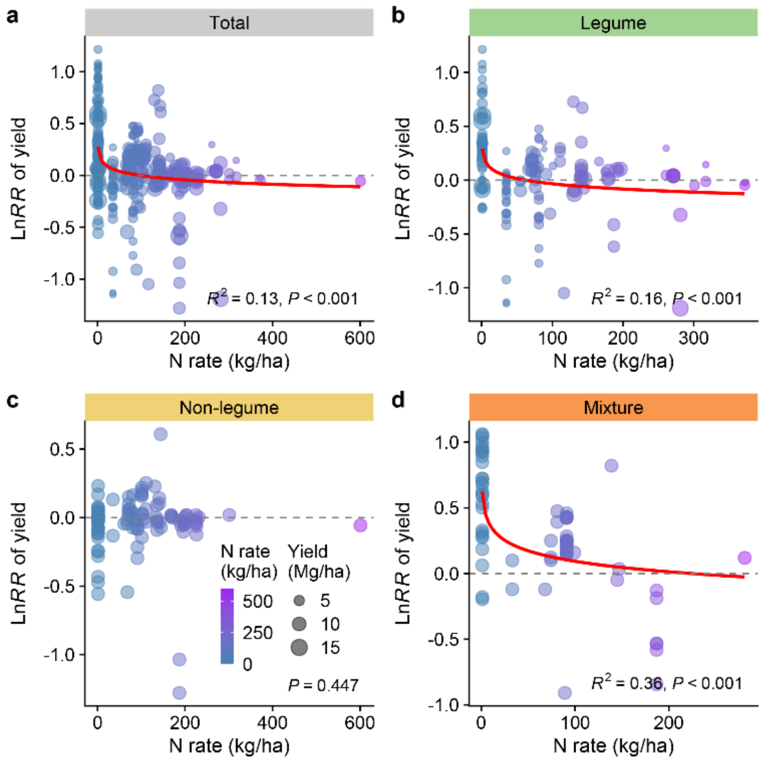

Supplementary Figure 11 Nonlinear decline of yield gain with excess N fertilizer rate. Relationships under total (a), legume (b), non-legume (c), and mixture (d) types of CCs. Red solid lines denote the significant correlations. Dot sizes are the actual crop yields under CC practices. Color scale indicate the rate of N fertilizer application.

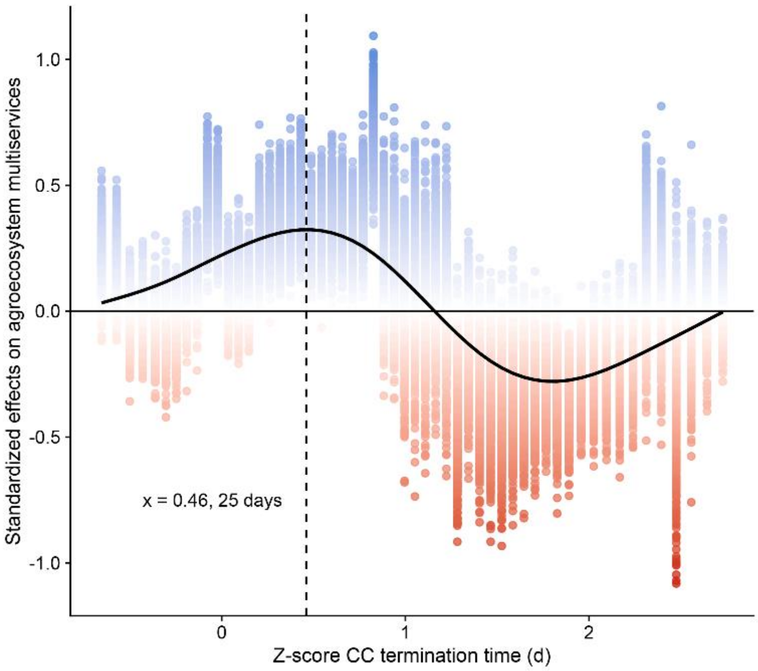

Supplementary Figure 12 Moving windows analysis demonstrating the nonlinear relationship of standardized effects of CC termination time and environmental factors on agroecosystem multiservices. The window size is 30 consecutive observations. Blue and red dots indicate positive and negative standardized effects, respectively. Black solid line denotes the correlation trend fitted by a generalized additive model incorporating CC termination time, climate, soil, microbe, and their multi-order interactions. Z-score represents the CC termination time (d) after z-score normalization. Source data are provided as a Source Data file.

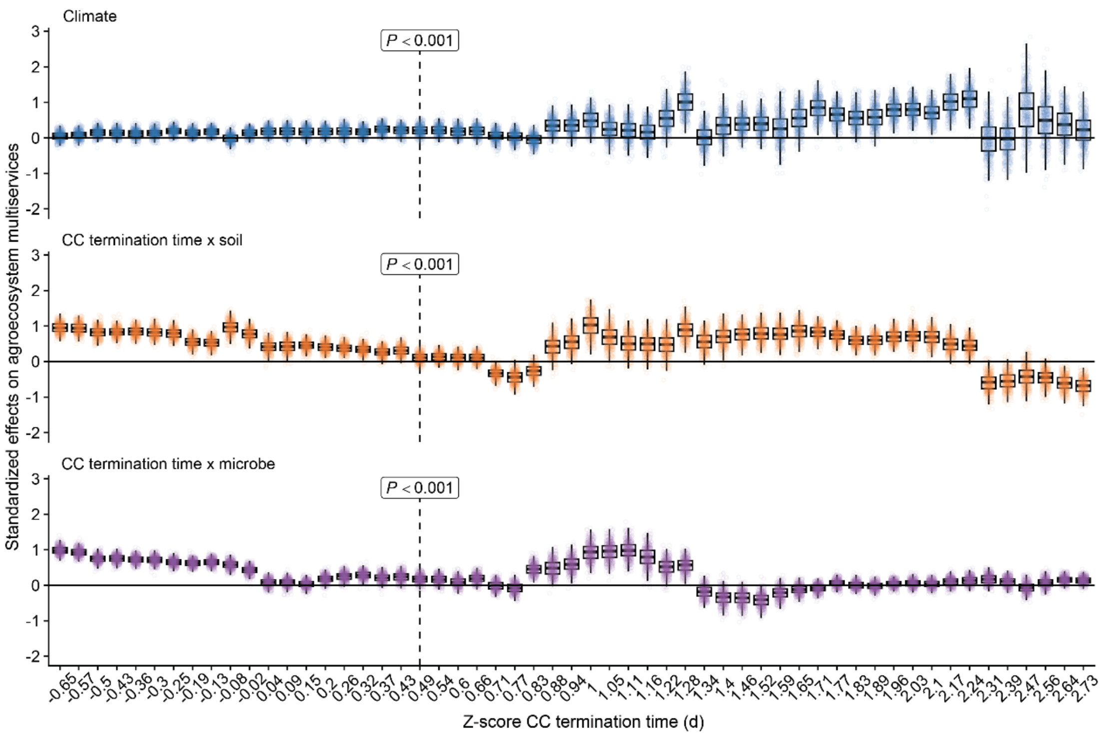

Supplementary Figure 13 Distribution of standardized interactive effects of CC termination time and environmental factors on agroecosystem multiservices (n = 500). Boxplots show the median, 25th and 75th percentiles of each distribution. Z-score represents the CC termination time (d) after z-score normalization. Source data are provided as a Source Data file.

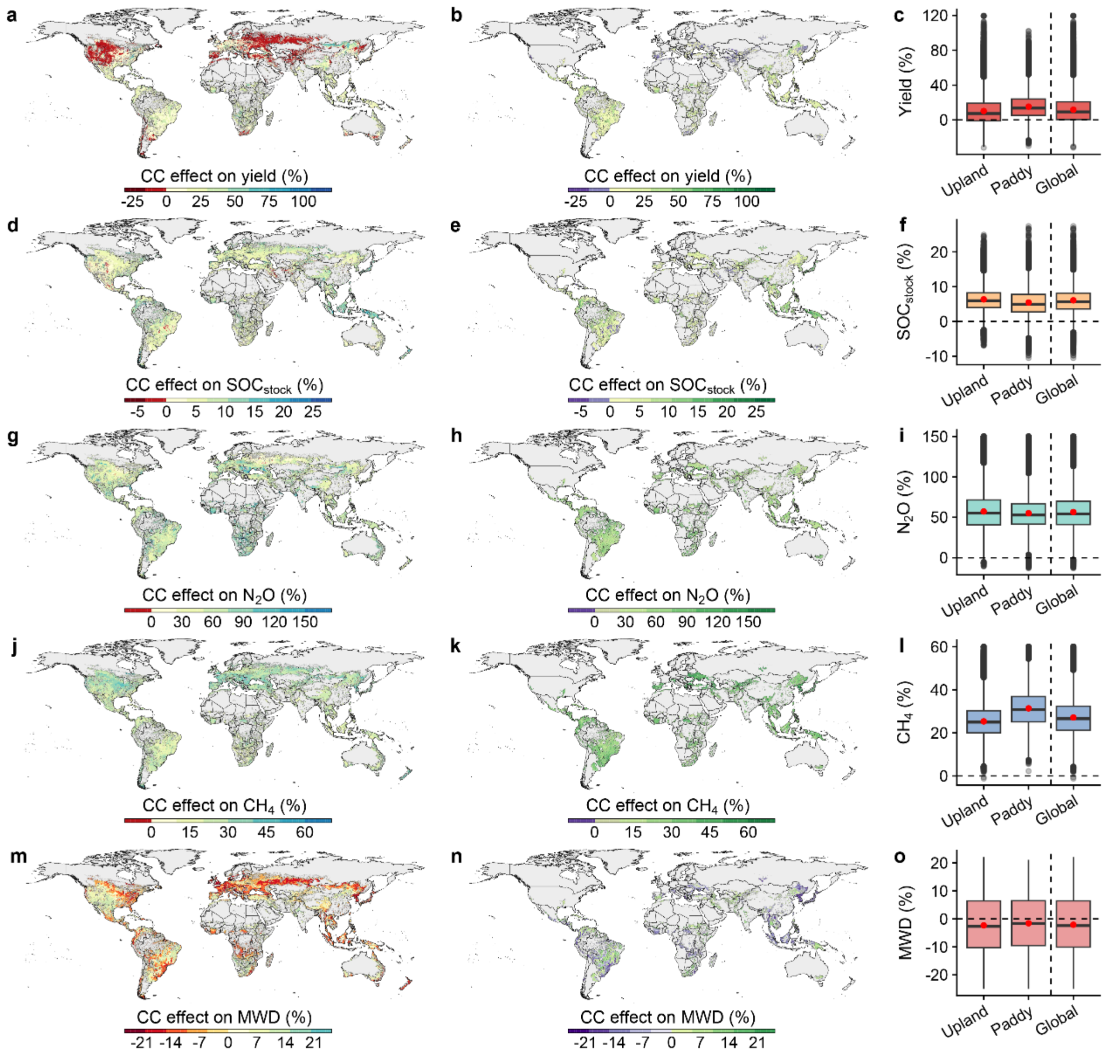

Supplementary Figure 14 Global pattern of CC effects (%) on five agroecosystem services with the optimal CC portfolio under the current scenario (2020). Distribution of CC effects in upland (a, d, g, j, m) and paddy (b, e, h, k, n), respectively. Boxplots show the median, 25th and 75th percentiles, and outliers of each cropland type or globe (c, f, i, l, o), with red dots indicating the mean values. *n* = 476,105 and 199,449 gridded values for upland and paddy respectively, with a total of 675,554 gridded values for globe.

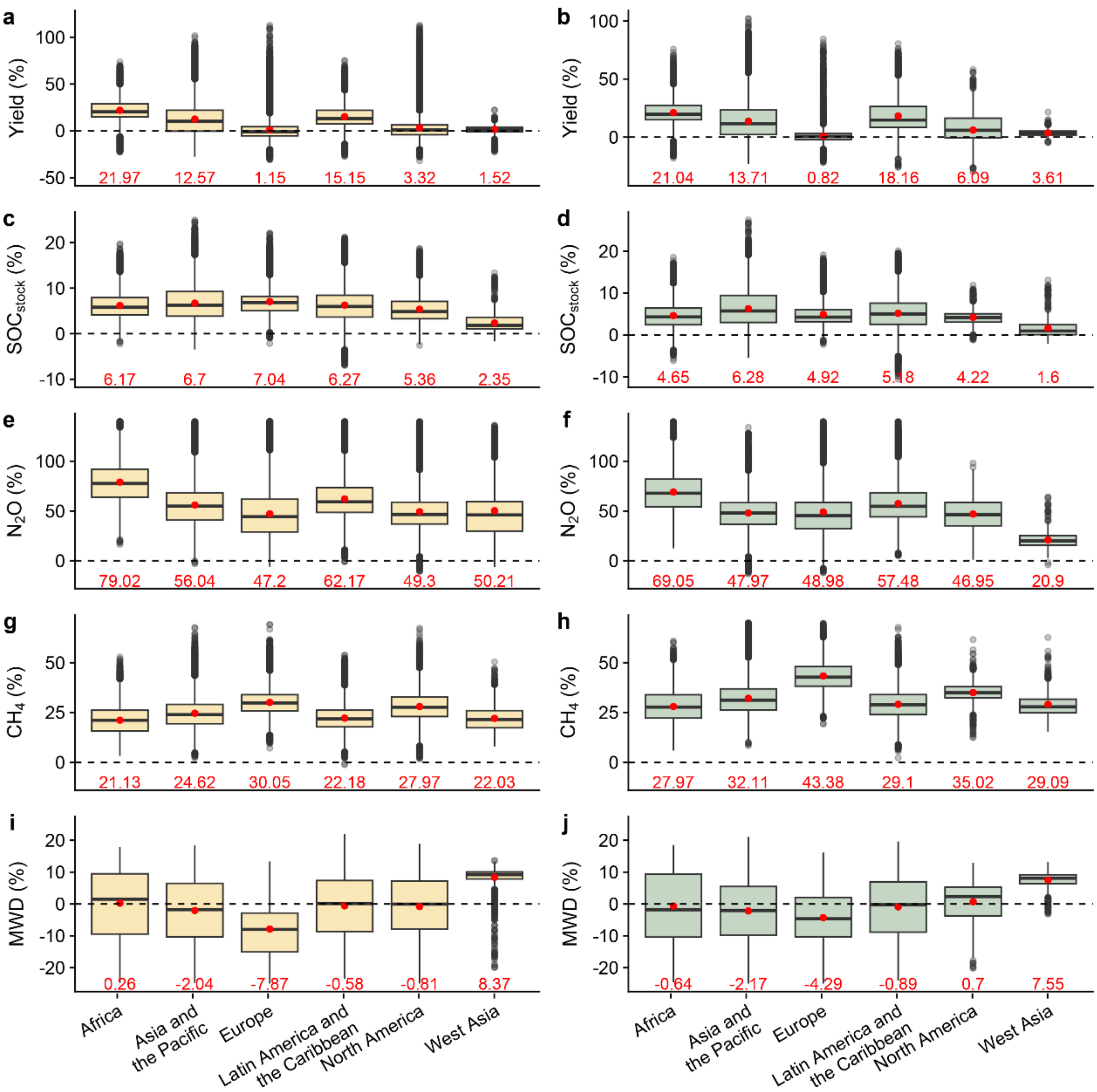

Supplementary Figure 15 Regional distribution of CC effects (%) on five agroecosystem services with the optimal CC portfolio for upland (a, c, e, g, i) and paddy (b, d, f, h, j) under the current scenario (2020). Boxplots show the median, 25th and 75th percentiles and outliers of each region, with red dots and numbers below indicating the mean values.

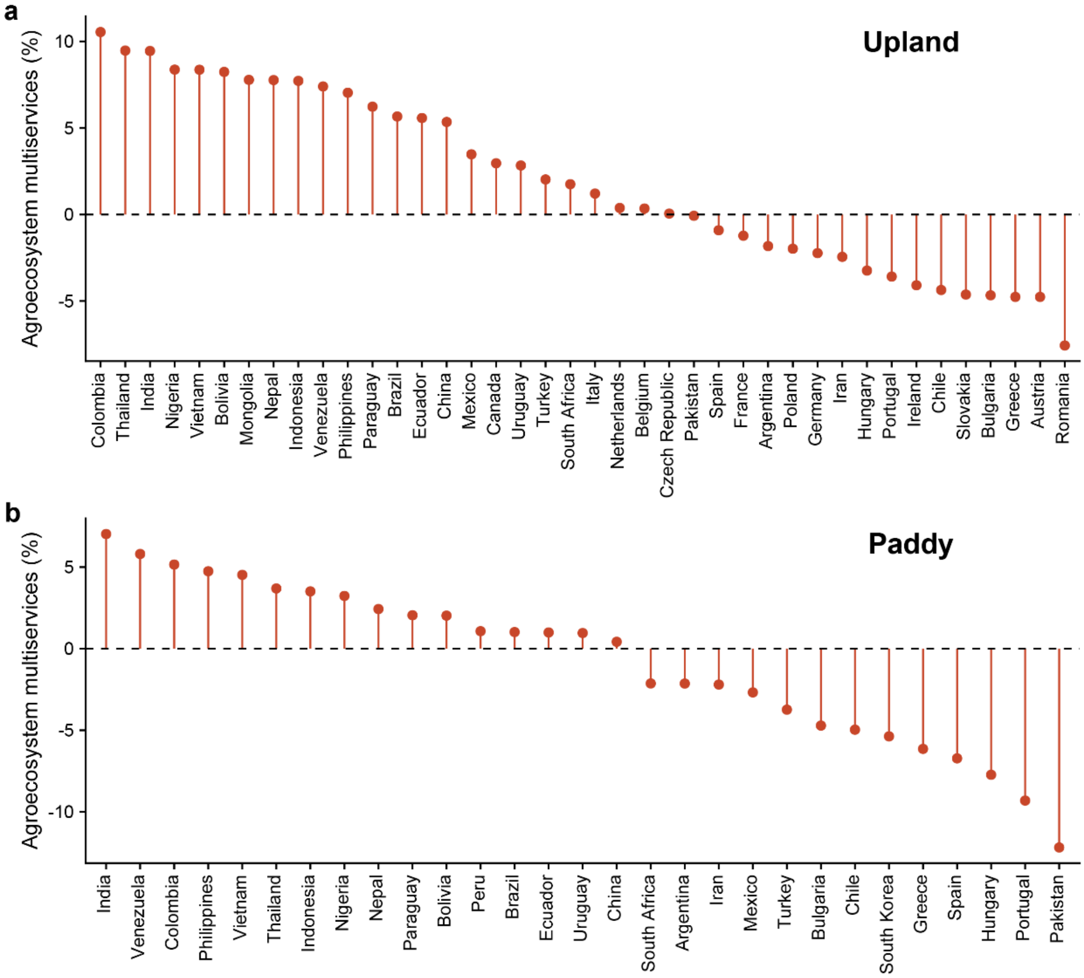

Supplementary Figure 16 Ranking of national CC benefits for agroecosystem services (%) with the optimal CC portfolio for upland (a) and paddy (b) under the current scenario (2020).

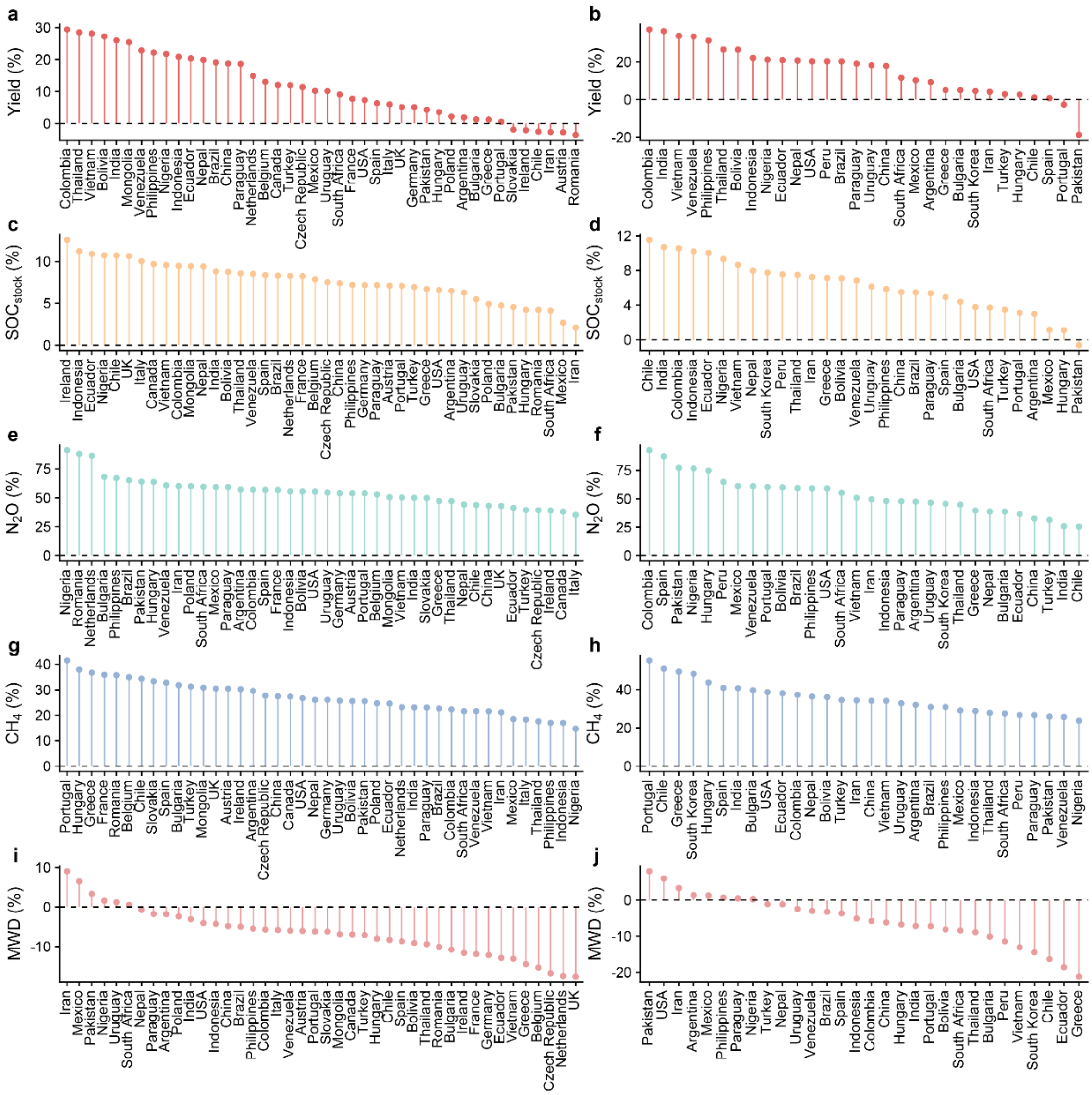

Supplementary Figure 17 Ranking of national CC effects (%) on five agroecosystem services with the optimal CC portfolio for upland (a, c, e, g, i) and paddy (b, d, f, h, j) under the current scenario (2020).

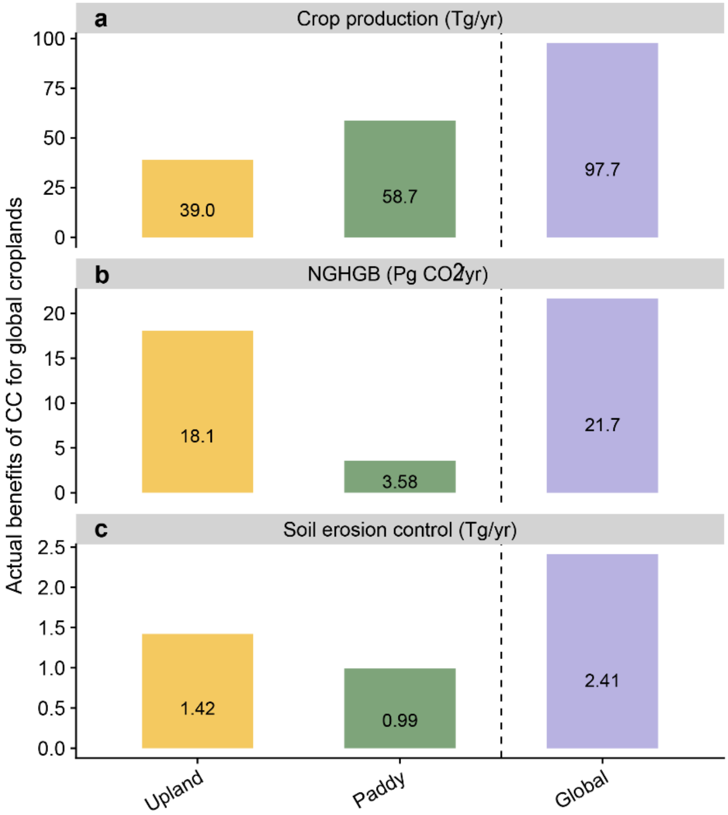

Supplementary Figure 18 Actual benefits of CC practices on crop production (a), net GHG budget (b) and soil erosion control (c) for global croplands. Because of the importance of duration, the estimation period of soil erosion control (Tg yr^{-1}) is during 2021–2030. Numbers in the columns represent individual average values.

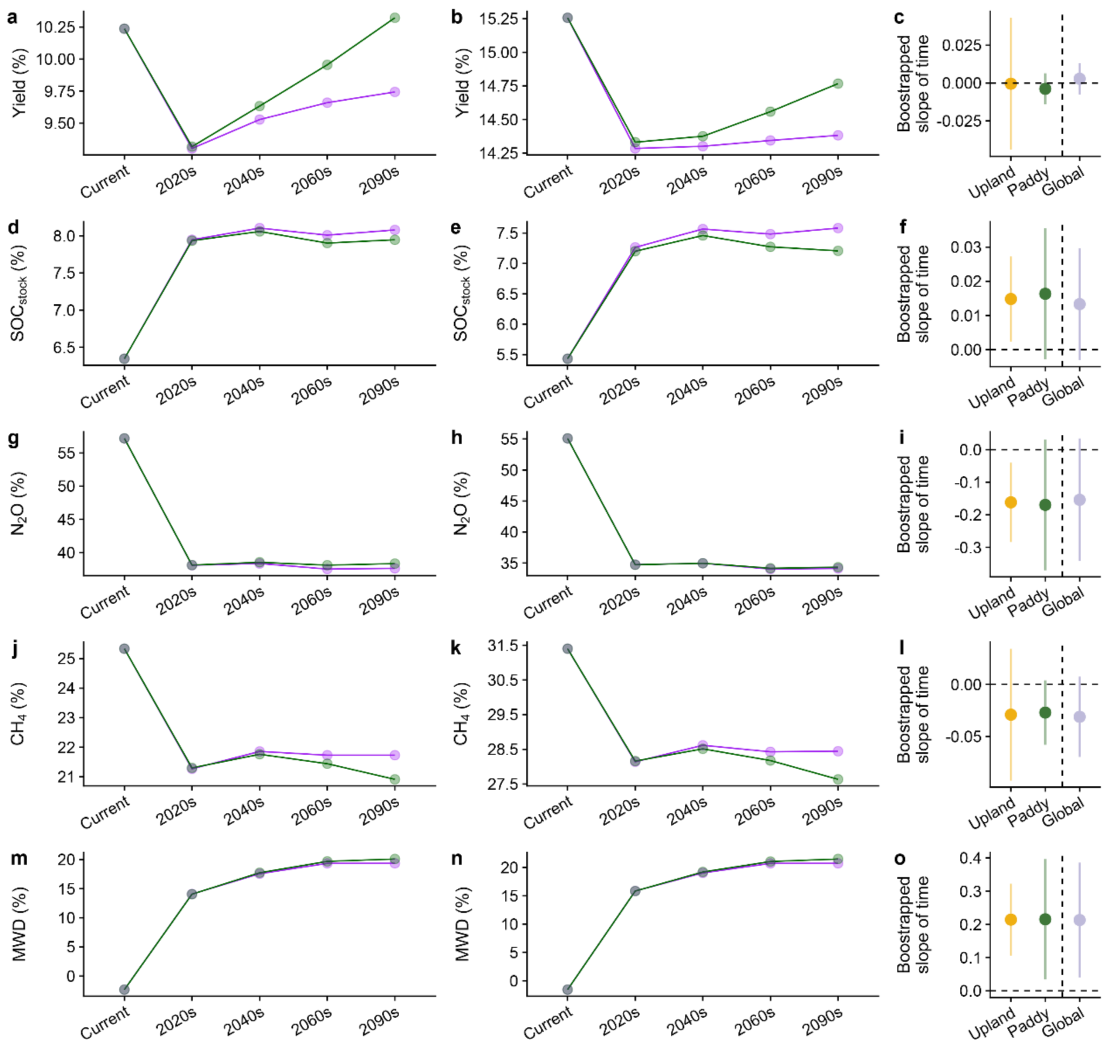

Supplementary Figure 19 Temporal trend of global CC effects (%) on five agroecosystem services with the optimal CC portfolio for upland (a, d, g, j, m) and paddy (b, e, h, k, n) from 2020 to 2100 under two climate emission scenarios (SSP126 and SSP370). Dots in c, f, i, l, o represent bootstrapped slopes of time versus CC effects and their 95% confidence intervals for each cropland type or globe.

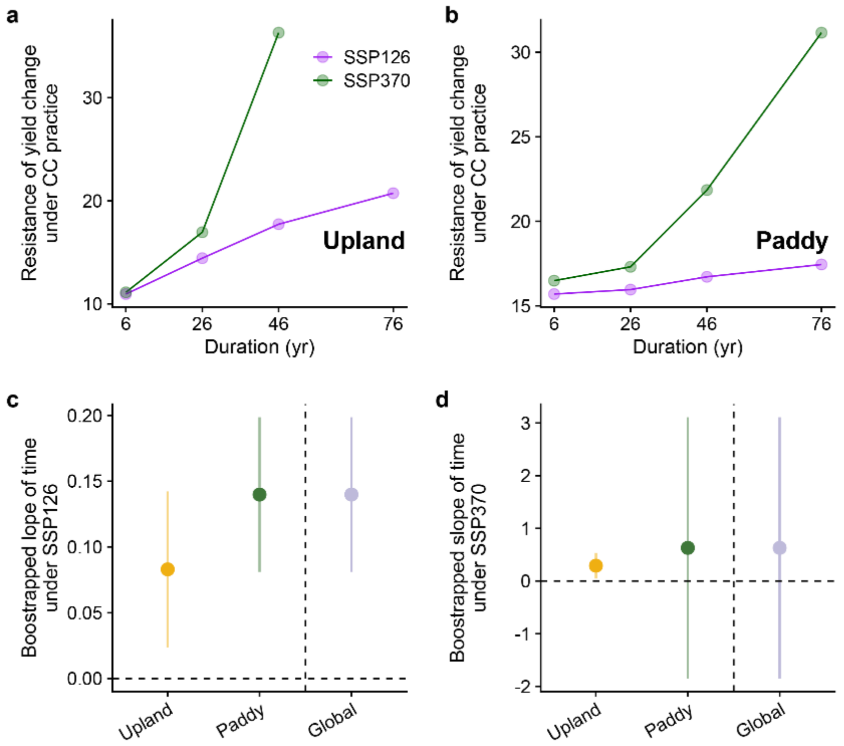

Supplementary Figure 20 Temporal trend of climatic resistance of yield loss under CC practices in SSP126 and SSP370 for uplands (a) and paddies (b). Bootstrapped regression slopes of time (duration) versus climatic resistance and their 95% confidence intervals under the scenarios of SSP126 and SSP370 are shown in (c) and (d), respectively.

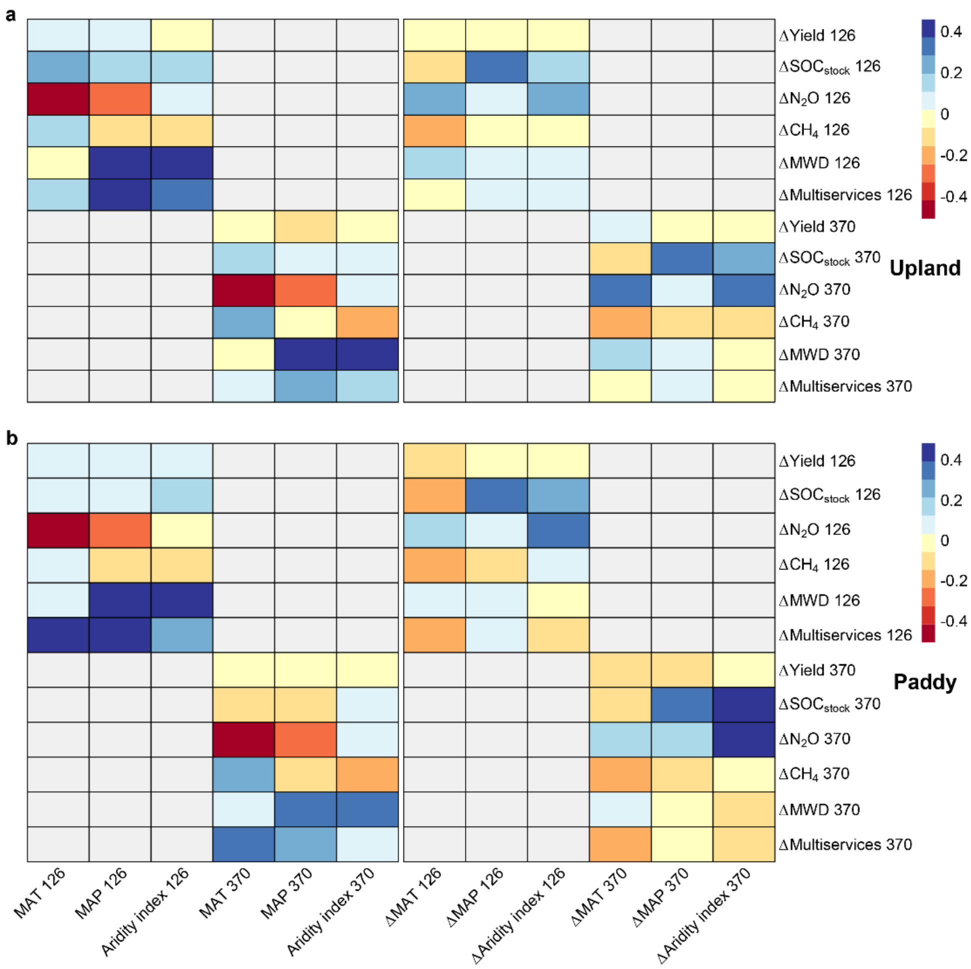

Supplementary Figure 21 Contribution of future climate variables and their changes to projected changes in agroecosystem services under CC practices. Corresponding relationships for uplands and paddy fields are shown in a and b, respectively. Δ, change in a given variable by century's end, denoting the difference between 2091–2100 and current (2020) in two climate emission scenarios (SSP126 and SSP370). The discrete color scale indicates the Pearson's correlation coefficient. Gray areas are unidentified relationships under two mismatched climate scenarios.

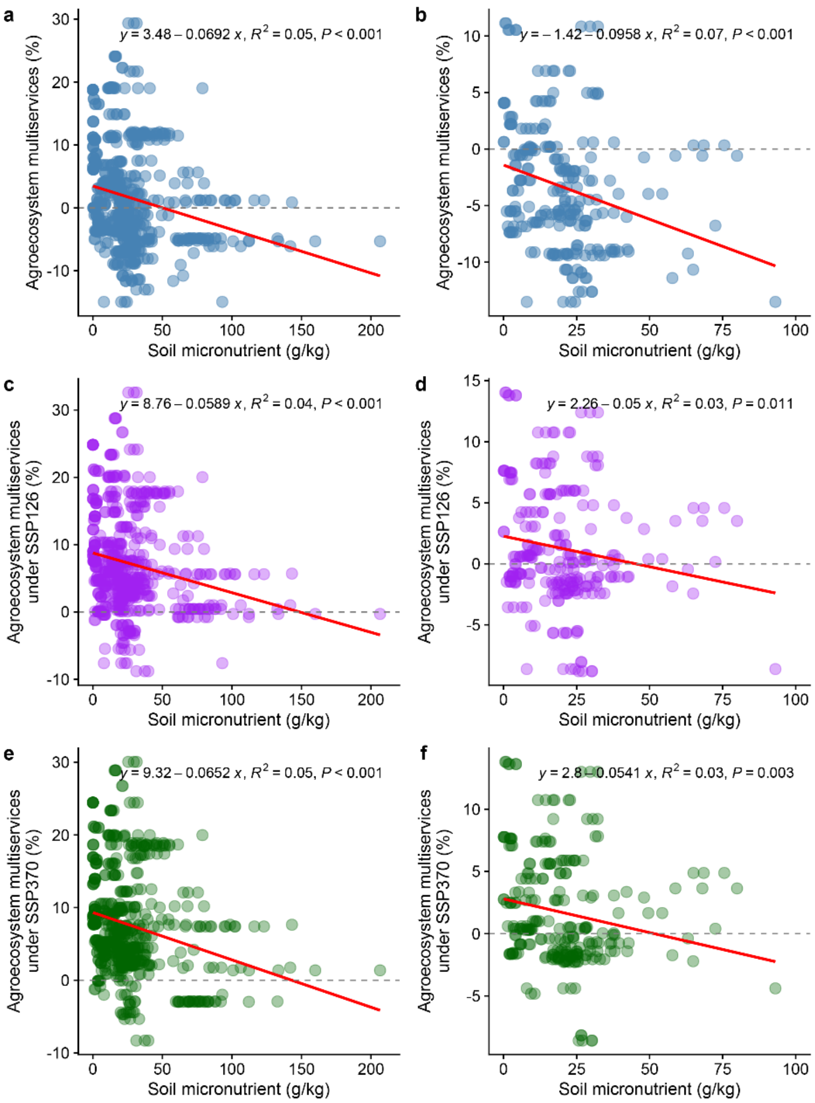

Supplementary Figure 22 Larger benefits of CCs for agroecosystem multiservices in areas with less soil micronutrients (n = 1,306). Linear relationships under three scenarios in uplands (a, c, e) and paddies (b, d, f), respectively. Soil micronutrient (g kg^{-1}) is the sum of copper, iron, manganese, zinc, cobalt, and nickel. Red solid lines denote the significant correlations. Source data are provided as a Source Data file.

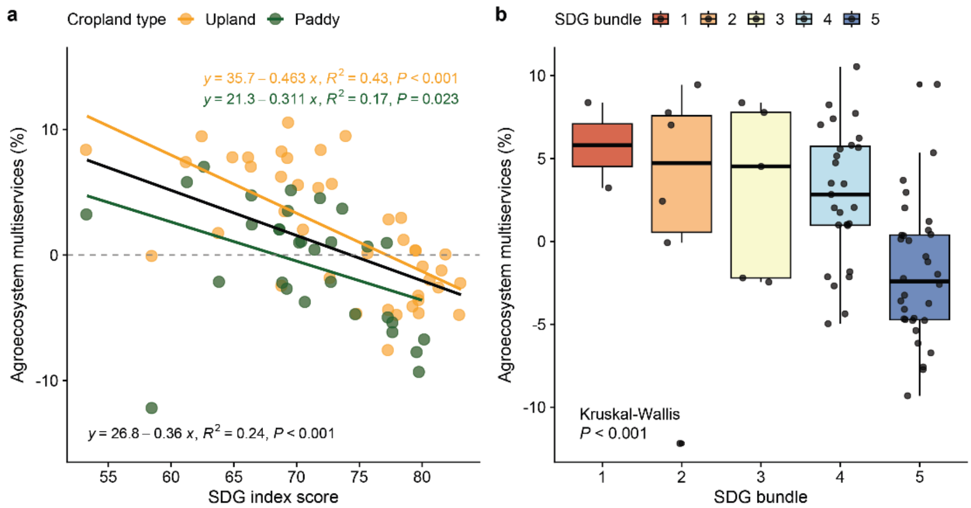

Supplementary Figure 23 Relationship of CC benefits with national sustainable development levels. (a) Black and color solid lines denote the significant correlations in general and different cropland types, respectively. $n = 42$ national SDG scores for upland and $n = 30$ national SDG scores for paddy. (b) National CC benefits within bundle 1 (nations with lowest development and good environment), bundle 2 (nations with low development and degraded environment), bundle 3 (nations with middle development while needing environment and climate action), bundle 4 (nations with middle development, inequality, and degraded environment), and bundle 5 (nations with high development while needing climate action). Boxplots show the median (center line), the interquartile range between the first and third quartiles (box bounds), whiskers extending to 1.5 times the interquartile range from the quartiles, and any points beyond this range as outliers. Significance of CC benefits for agroecosystem multiservices ($P < 0.001$) among different bundles has been tested using Kruskal-Wallis test. Source data are provided as a Source Data file.

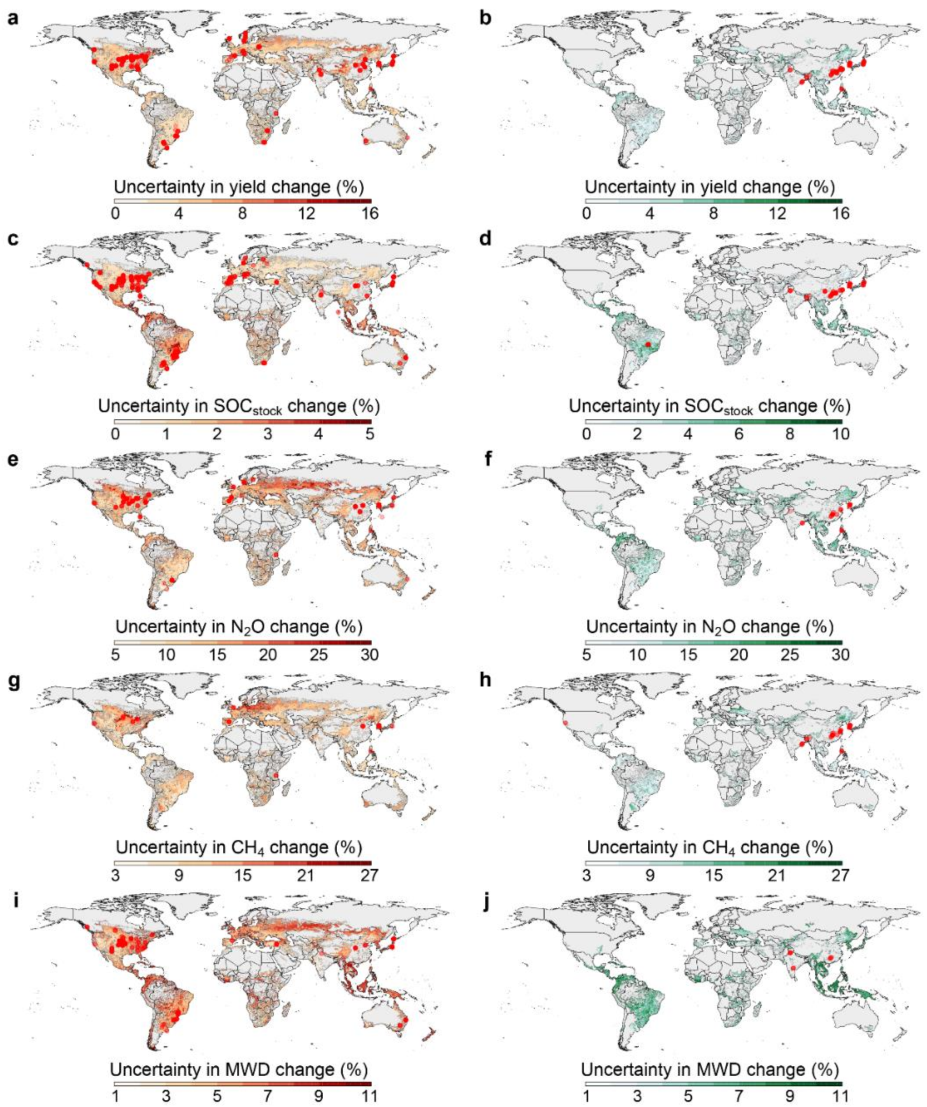

Supplementary Figure 24 Global distribution of standard errors in scale-up CC effects (%) for upland (a, c, e, g, i) and paddy (b, d, f, h, j). n = 476,105 and 199,449 gridded values for upland and paddy respectively. Red dots represent the location of studies for each agroecosystem services included in our dataset.

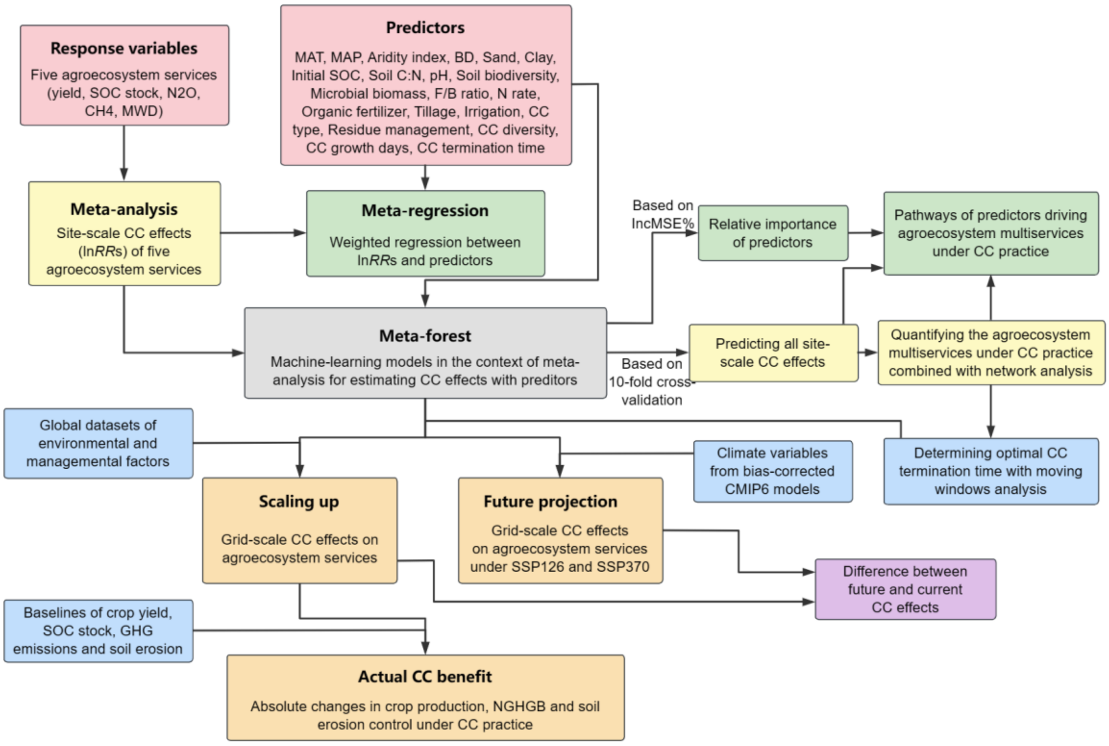

Supplementary Figure 25 Working procedure for quantifying and evaluating the CC benefits to agroecosystem services.

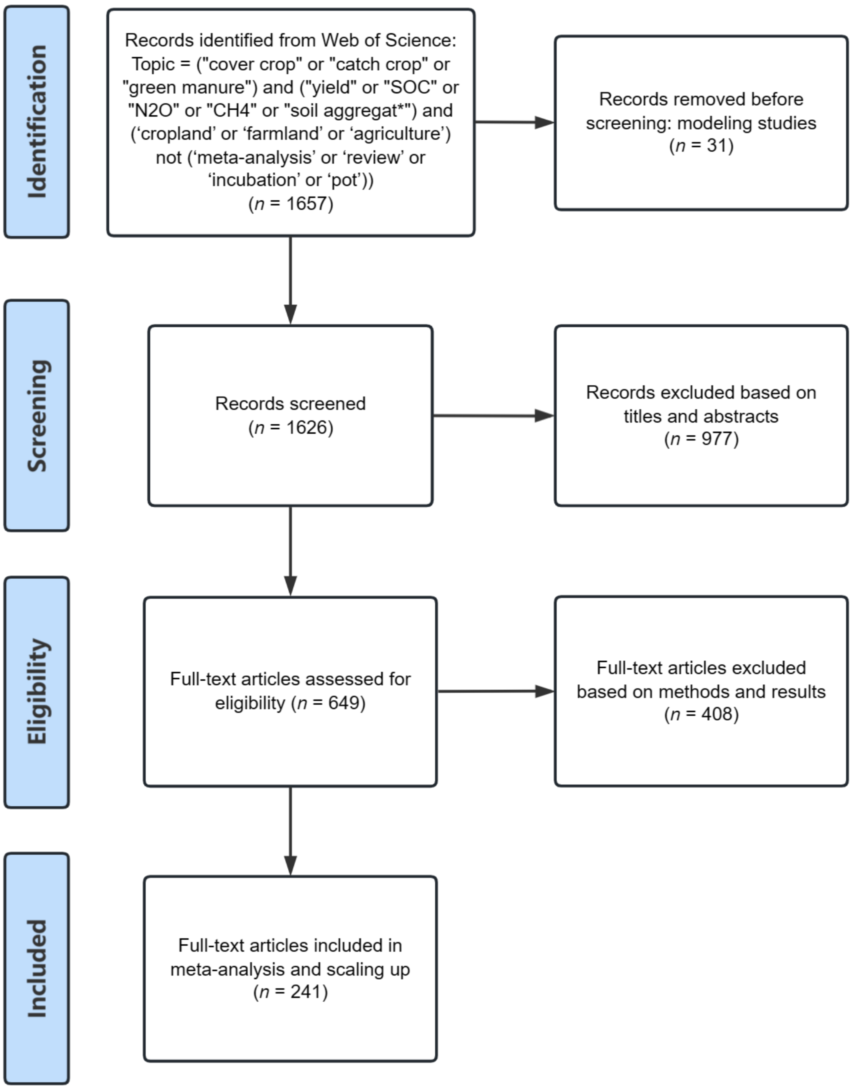

Supplementary Figure 26 PRISMA flowchart for the meta-analysis in this study.

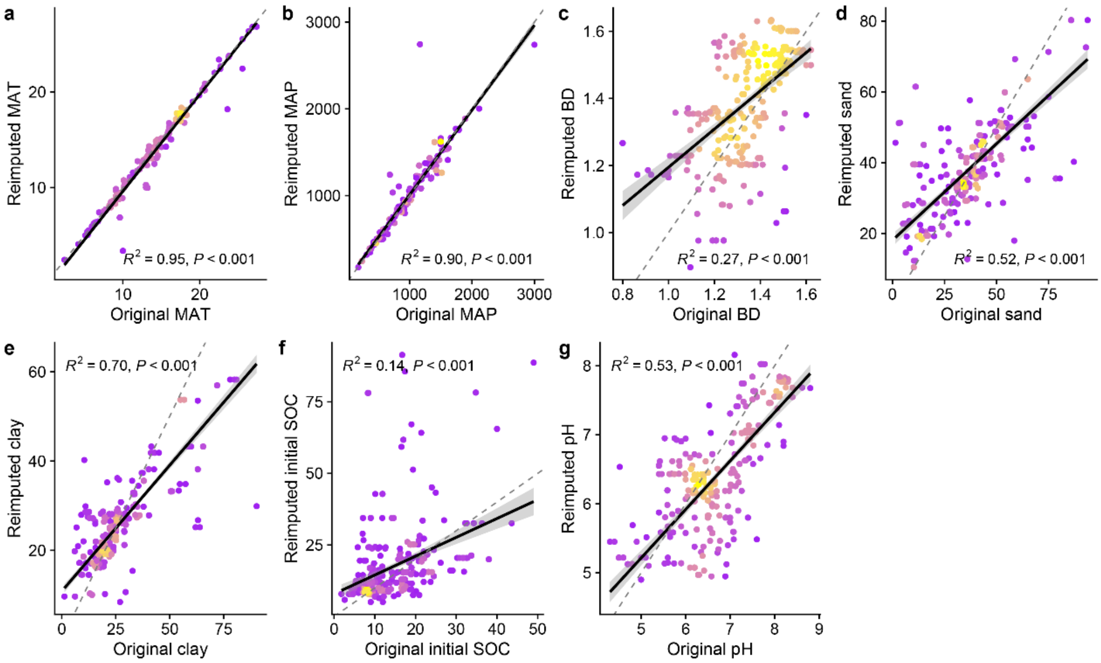

Supplementary Figure 27 Sensitivity analysis (random missing value imputation) of filling missing values of environmental factors with high-resolution global maps. Environmental factors include mean annual temperature (a), mean annual precipitation (b), soil bulk density (c), sand content (d), clay content (e), soil organic carbon (f), and pH (g). Black solid lines denote the significant correlations.

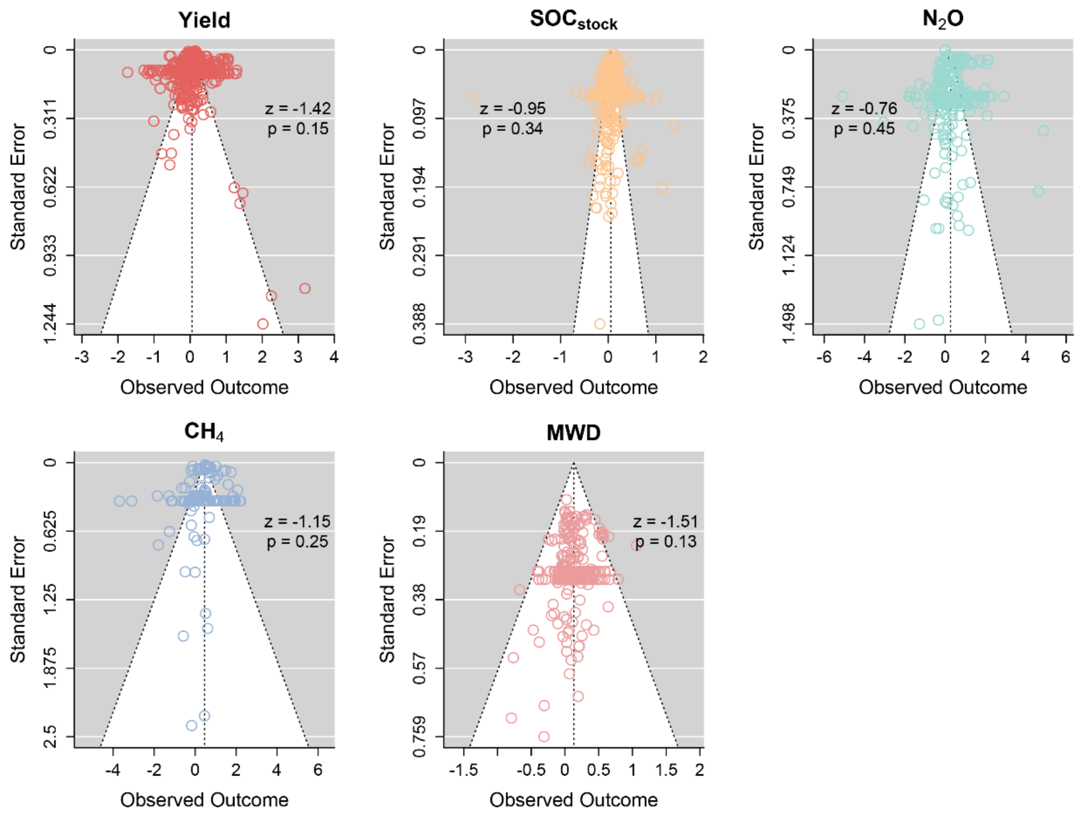

Supplementary Figure 28 Funnel plots showing the presence or absence of publication bias. $P > 0.05$ denotes no publication bias according to Egger's regression.

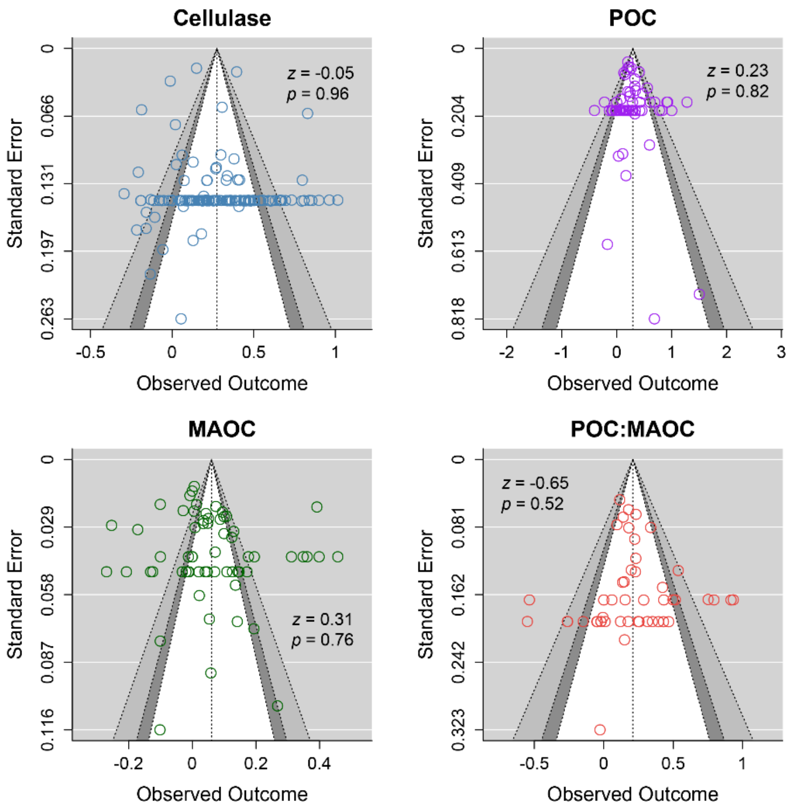

Supplementary Figure 29 Funnel plots illustrating the absence of publication bias within the long-term field data. $P > 0.05$ denotes no publication bias according to Egger's regression.

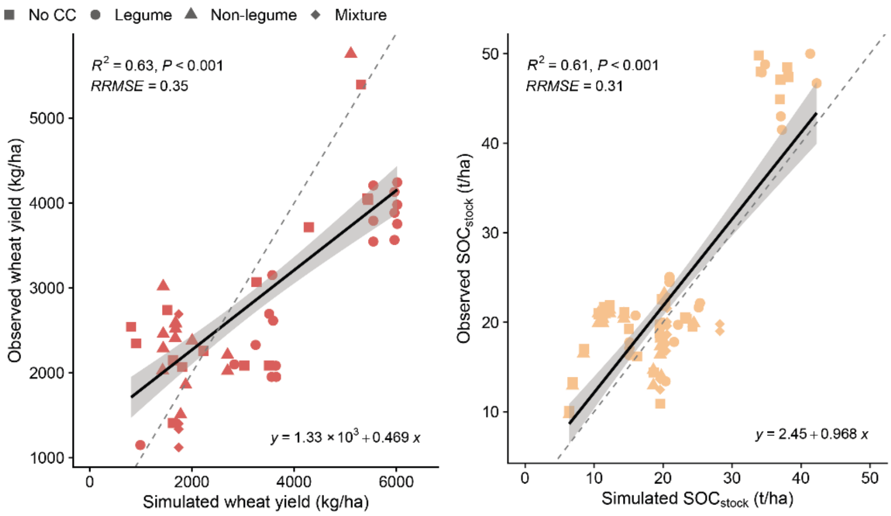

Supplementary Figure 30 Predictive performance of simulations from APSIM model. Different shapes of points represent four CC scenarios. Black solid lines denote the significant correlations. RRMSE, relative root mean square error.

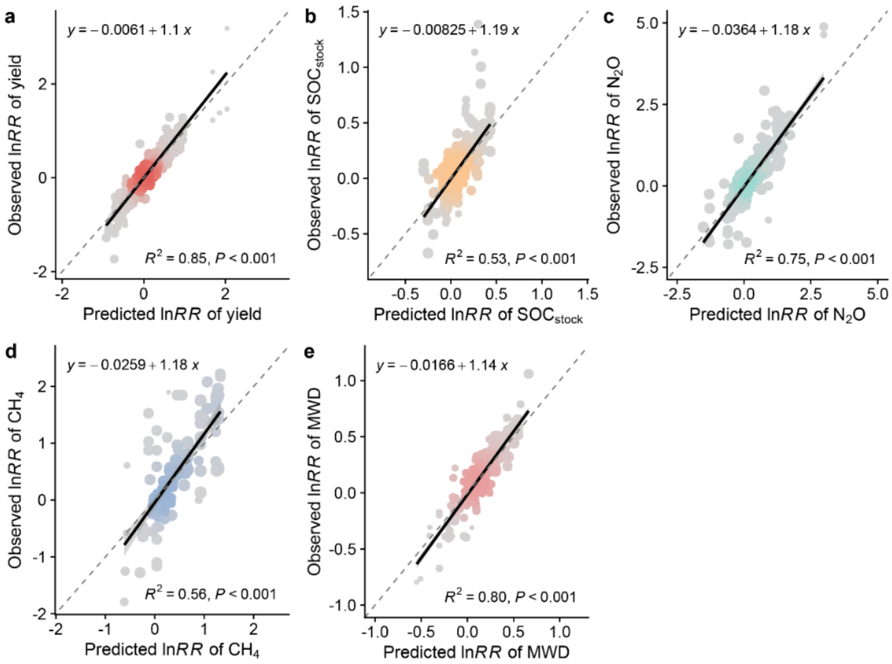

Supplementary Figure 31 Fitting performance of MF predictions for five agroecosystem services, including yield (a), SOC stock (b), N_2O (c), CH_4 (d), and MWD (e). Dark colors from gray to color represent the increasing density. Black solid lines denote the significant correlations, with dot sizes proportional to model weights.

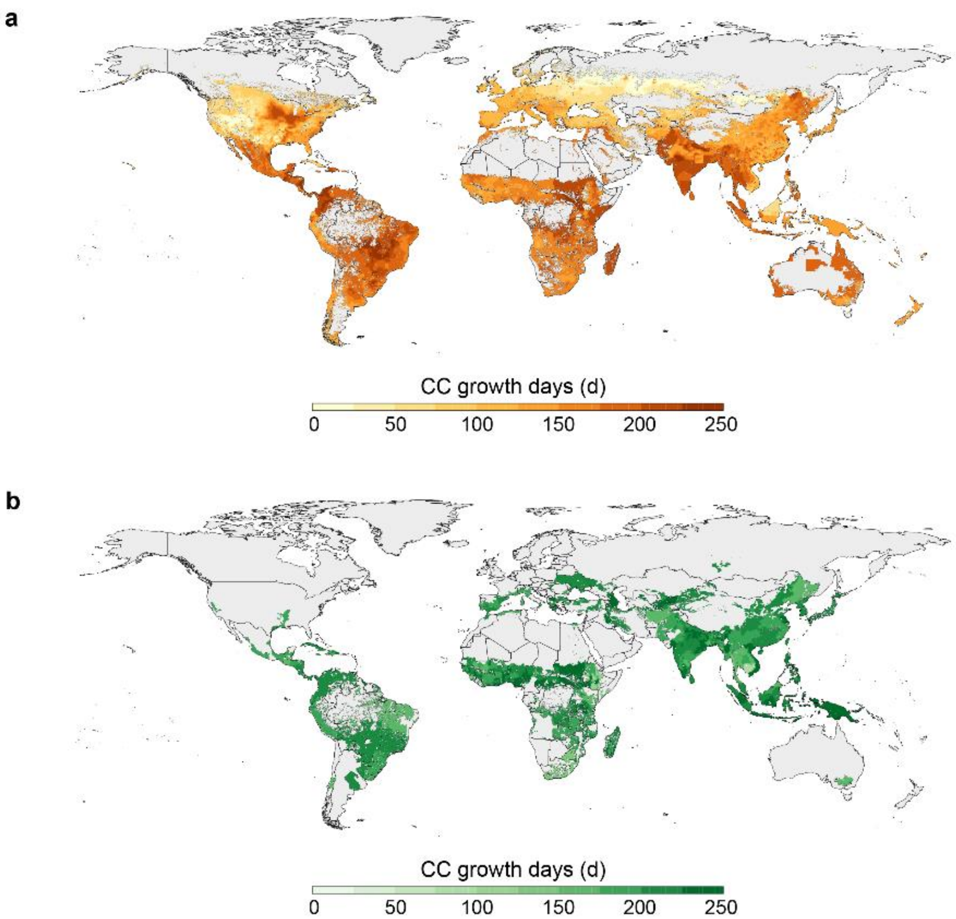

Supplementary Figure 32 Estimated CC growth days based on the optimal CC termination time (25 days) and growth days of main crops from GGCMI Phase 3. CC growth days for upland and paddy fields are shown in a and b, respectively.